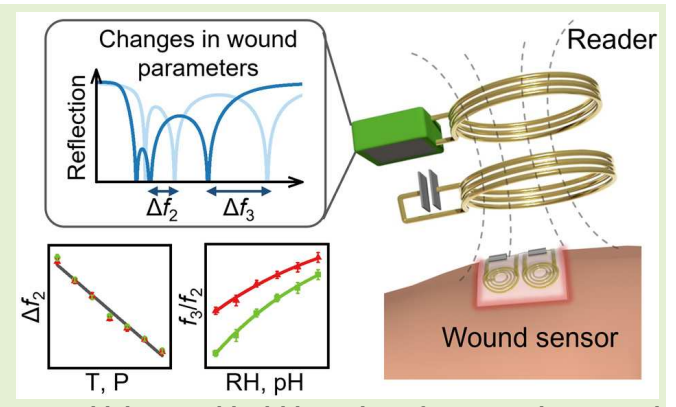


Multimodal Wireless Wound Sensors via Higher-Order Parity-Time Symmetry

Zhilu Ye[®], Minye Yang[®], Mohamed Farhat[®], Mark M.-C. Cheng, *Senior Member, IEEE*, and Pai-Yen Chen[®]. *Senior Member, IEEE*

Abstract—Chronic wounds have emerged as a significant healthcare burden, affecting millions of patients worldwide and presenting a substantial challenge to healthcare systems. The diagnosis and management of chronic wounds are notably intricate, with inappropriate management contributing significantly to the amputation of limbs. In this work, we propose a compact, wireless, battery-free, and multimodal wound monitoring system to facilitate timely and effective wound treatment. The design of this monitoring system draws on the principles of higher-order parity-time (PT) symmetry, which incorporates spatially balanced gain, neutral, and loss, embodied by an active –RLC reader, an LC intermediator, and a passive RLC sensor, respectively. Our experimental results demonstrate that this wireless wound sensor can detect temperature (T), relative humidity (RH),



pressure (P), and pH with exceptional sensitivity and robustness, which are critical biomarkers for assessing wound healing status. Our in vitro experiments further validate the reliable sensing performance of the wound sensor on human skin and fish. This multifunctional monitoring system may provide a promising solution for the development of futuristic wearable sensors and integrated biomedical microsystems.

Index Terms— Biomedical sensors, parity-time (PT) symmetry, wearable sensors, wireless sensors, wound healing.

I. INTRODUCTION

EARABLE sensors that monitor the physical and chemical conditions of the human body have gained increasing importance in the past decade [1], [2], [3], [4], [5]. To date, various wearable sensors, such as glucose sensors [1], blood pressure sensors [2], and electrocardiogram sensors [3], [4], have been proposed to assist clinical decision making, treatment, and health management. Despite these recent advances, relatively less attention has been paid to chronic

Manuscript received 15 September 2023; accepted 10 November 2023. Date of publication 21 November 2023; date of current version 2 January 2024. This work was supported in part by the National Science Foundation under Grant ECCS-CCSS 1914420 and in part by the National Institute of Health under Grant R01EB033371. The associate editor coordinating the review of this article and approving it for publication was Dr. Jurgen Kosel. (Corresponding author: Pai-Yen Chen.)

Zhilu Ye, Minye Yang, and Pai-Yen Chen are with the Department of Electrical and Computer Engineering, University of Illinois at Chicago, Chicago, IL 60607 USA (e-mail: zye27@uic.edu; myang66@uic.edu; pychen@uic.edu).

Mohamed Farhat is with the Division of Computer Electrical and Mathematical Sciences and Engineering, King Abdullah University of Science and Technology (KAUST), Thuwal 23955-6900, Saudi Arabia (e-mail: Mohamed.farhat@kaust.edu.sa).

Mark M.-C. Cheng is with the Department of Electrical and Computer Engineering, University of Alabama, Tuscaloosa, AL 35487 USA (e-mail: mmcheng@ua.edu).

Digital Object Identifier 10.1109/JSEN.2023.3333292

wound monitoring. Chronic wounds that fail to heal in an orderly manner within expected timeframes affect more than 6.5 million people in the United States alone and cost the economy over \$25 billion annually [6], [7]. This burden is still surging due to the rising prevalence of obesity, diabetes, and aging population [6], [7]. In current clinical practice, wound assessment relies primarily on the visual inspection of the wound size and depth, as well as signs of inflammation [8]. The reliability of visual assessment depends largely on the experience of clinicians and is inevitably influenced by a degree of subjectivity. Especially for chronic wounds whose early symptoms are subtle and difficult to distinguish from those of normally healing wounds, the traditional assessment method may fail to provide sufficient information of the wound, leading to improper or delayed treatment. Recently, researchers have disclosed the underlying relationship between wound status and various pivotal biomarkers (e.g., temperature, moisture, pH, strain, and oxygen levels) [9], [10], [11], [12], [13], [14]. Monitoring these physiological parameters may provide a more quantitative evaluation of the wound healing process and allow for more rapid and accurate diagnosis of chronic wounds.

In this context, a plethora of wearable biosensors have been developed to effectively monitor temperature [9], [10], humidity [11], [12], and other crucial parameters in the vicinity

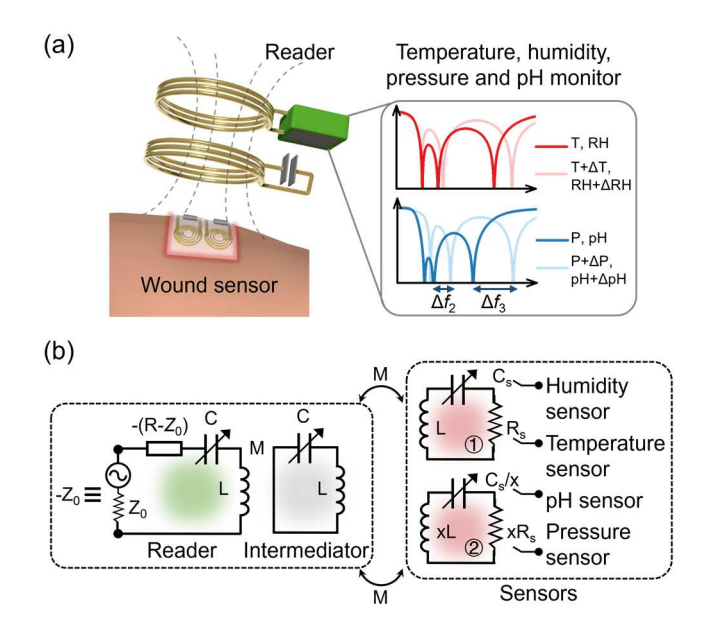


Fig. 1. (a) Schematic of the wireless wound monitoring system, where the parameters to be detected (e.g., temperature, RH, pressure, and pH) are obtained from the shifts of narrow resonant dips. (b) Equivalent circuit diagram of the third-order PTX-symmetric sensing system, which consists of an active -RLC reader, an LC intermediator, and passive RLC sensors.

of the wound site [7], [13], [14]. The objective, sensor-based assessment is definitely an immense improvement compared with conventional methods. Yet, most reported wound sensors still suffer from one or more critical limitations, such as high manufacturing cost, insufficient sensitivity, unavoidable battery usage, and redundant wire connections linking sensors to external reading equipment (which restrict the activities of patients) [15], [16], [17], [18]. Moreover, some of the sensing systems can only detect a single parameter of wound healing [14], [19], [20], [21], which is obviously inadequate since wound healing is a complex and multistage process accompanied by dynamic changes in multiple physiological parameters. To address the existing limitations, we present a battery-free, multiplex sensing platform for monitoring the wound healing process. The platform leverages the concept of generalized higher-order parity-time (PT) symmetry [22], [23], [24], [25]. As depicted in Fig. 1(a), the wound site parameters, including temperature (T), relative humidity (RH), pressure (P), and pH level, can be captured by detecting the resonant dip shifts in the reflection spectrum. These measured indicators are important for assessing the wound status. Typically, normal skin or a healing wound has a temperature of 30.2 °C-36.9 °C and a slightly acidic pH of 5.0-6.5, while an infected wound experiences a suddenly increased temperature and a slightly basic pH (above 7.4) due to the presence of certain types of enzymes and bacteria [19], [20], [26], [27]. Moisture is a parameter that must be carefully managed in the wound environment, since dry wounds usually show a slower epithelialization, while moist wounds may have an increased risk of infection [28]. Pressure is predominantly linked to cell proliferation and neovascularization [11].

In this article, we present a systematic theoretical study and experimental demonstration of the generalized higher-order

PT-symmetric wound sensing system, which can monitor multiple wound healing indicators with excellent sensitivity. Although PT-symmetric telemetry has been applied to several wireless sensing applications, experimental demonstrations to date have been detecting single resistive or reactive change on the sensor [29], [30], [31]. To the best of our knowledge, this is the first time that multiple physiological parameters are sensed at the time using the PT-symmetric telemetry. In this work, we experimentally verify that a PT-symmetric wound sensor can be used to simultaneously monitor temperature (20 °C–50 °C), RH (30%–90%), pH (4–10), and pressure (0-200 mmHg). The sensing ranges are carefully designed to cover all possible environmental conditions surrounding a wound or surgical site. The proposed PT-symmetric multimodal sensing platform enables a myriad of healthcare applications, such as wound management, wearable Internet of Things (IoT) devices, biotelemetry, and telemedicine.

II. THEORETICAL ANALYSIS

PT symmetry is an essential milestone in non-Hermitian physics, unveiling that nonconservative Hamiltonians that satisfy parity (P) and time-reversal (T) operators can possess completely real eigenspectra [29], [32], [33]. This revolutionary discovery has made an enormous difference in the fields of optics [34], [35], electronics [34], [36], [37], electromagnetics [38], [39], [40], [41], and acoustics [42]. Standard PT-symmetric electronic systems have shown significant advancements in sensing applications, exhibiting superior sensitivity compared to traditional *RLC* sensors [21], [23], [29], [37]. The enhanced sensitivity of the standard secondorder PT-symmetric system can be attributed to eigenfrequency bifurcation near the exceptional point (EP), which allows significant resonance frequency shift in response to small impedance perturbations. Despite their effectiveness in improving the sensing performance, the second-order PTsymmetric system can only detect one type of resistive or reactive change. The third (or higher)-order PT-symmetric telemetry with more than three eigenfrequencies offers a greater degree of freedom in data interpretation. Furthermore, PT-reciprocal scaling (PTX) symmetry has been introduced as a generalized form of PT symmetry [23], [39], [43]. In principle, PT-symmetric systems necessitate a precise balance of gain and loss, whereas such a weak constraint can be removed in the PTX-symmetric systems, even though PT and PTX systems share the same eigenspectrum but different eigenmodes [23]. Hence, PTX-symmetric systems may provide more design degrees of freedom.

Fig. 1(b) shows the schematic of the generalized higher-order PT-symmetric wound sensing system, which comprises an active -RLC reader (gain), an LC intermediator (neutral), and two passive RLC sensors (loss). The two RLC tank sensors, which share the same reader, respectively, make the system fulfill the PT- and PTX-symmetric conditions. As shown in Fig. 1(b), the PTX-symmetric system is similar to its PT-symmetric counterpart, but with all elements in the tank sensor scaled in a specific manner (i.e., $R \to xR$, $L \to xL$, and $C \to x^{-1}C$, where x is the reciprocal scaling factor). Here, the PT sensor includes a thermistor and a capacitive

humidity sensor, and the PTX sensor consists of a resistive pressure sensor and a pH sensor. This telemetry system can simultaneously monitor the temperature, humidity, pressure, and pH at the wound site. The PT- and PTX-symmetric systems can be described by Kirchhoff's laws, which provide us with the effective non-Hermitian Hamiltonian $H_{\rm eff}$ of the system [23], [29], [36]. For the PT/PTX-symmetric system shown in Fig. 1(b), there exist eigenfrequencies, which can be obtained by letting $|H_{\rm eff} - \omega \mathbf{I}| = 0$. Under the PT/PTX-symmetric condition (i.e., $|-R| = R_s$, $C = C_s$), the three eigenfrequencies can be written as follows:

$$\omega_1 = \omega_0 \sqrt{\frac{2\gamma^2 - 1 - \sqrt{1 - 4\gamma^2 + 8\gamma^4 \kappa^2}}{2\gamma^2 (1 - 2\kappa^2)}}$$
 (1a)

$$\omega_2 = \omega_0 \Big(= 1/\sqrt{LC} \Big) \tag{1b}$$

$$\omega_3 = \omega_0 \sqrt{\frac{2\gamma^2 - 1 + \sqrt{1 - 4\gamma^2 + 8\gamma^4 \kappa^2}}{2\gamma^2 (1 - 2\kappa^2)}}$$
 (1c)

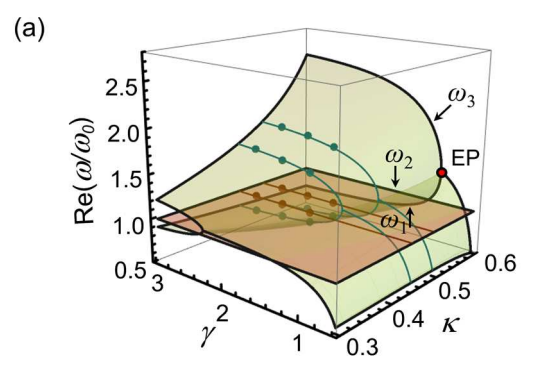
where γ denotes the gain-loss parameter or the effective Q-factor of the resonant tank ($\gamma = R^{-1}\sqrt{L/C}$), κ is the coupling coefficient between the neighboring resonators ($\kappa = M/L$, where M is the mutual inductance), and ω_0 is the resonant angular frequency of the neutral LC tank ($\omega_0 = 1/\sqrt{LC}$). We note that the PT- and PTX-symmetric systems share the same eigenfrequencies. The real parts of eigenfrequencies are plotted in Fig. 2(a), where the theoretical and experimental results are presented by colored contours and dots, respectively. In Fig. 2(a), an EP can be clearly observed at

$$\gamma_{\rm EP} = \sqrt{1 + \sqrt{1 - 2\kappa^2}} / (2\kappa) \tag{2}$$

where an eigenfrequency bifurcation occurs along the EP loci. When $\gamma > \gamma_{\rm EP}$, the system is in the exact *PT*-symmetric phase, whereby the eigenfrequencies are purely real and correspond to the resonant (angular) frequencies.

Fig. 2(b) shows the contours of reflection as a function of frequency and gain-loss parameter γ for the third-order PT/PTX-symmetric system, where the reflection minima occur at the eigenfrequencies (or resonant frequencies). Unlike the standard second-order PT- and PTX-symmetric systems that display dissimilar resonance line shapes [23], [43], the third-order PT- and PTX-symmetric systems possess exactly identical reflection spectra. Noticeably, the PTX system may offer wider design flexibility as it allows for adjusting/scaling the lumped element values on the sensor side. As evident from Fig. 2(a) and (b), when the system operates at the exact PTsymmetric phase, the two resonant frequencies, ω_1 and ω_3 , are sensitive to the gain-loss parameter γ and coupling coefficient κ . Especially when γ is around γ_{EP} , even a tiny resistive or reactive perturbation that alters γ can lead to noticeable shifts of ω_1 and ω_3 . On the other hand, the eigenfrequency ω_2 is fixed to ω_0 .

When monitoring wound parameters, the system experiences changes in both resistance and capacitance and should be able to distinguish between changes in each. These variations could slightly break the *PT/PTX* symmetry of the system. Considering a small resistive perturbation applied on



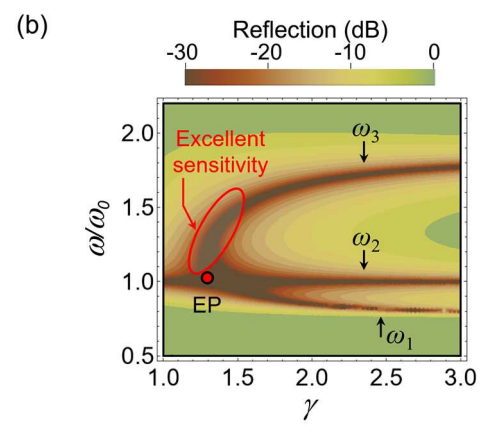


Fig. 2. (a) Real parts of eigenfrequencies of the *PT/PTX*-symmetric system in Fig. 1(b), where the calculated and measured results are represented by color contours and scattered points, respectively. (b) Contours of reflection coefficients as a function of the gain-loss parameter γ and the normalized angular frequency ω/ω_0 ; here, $\kappa=0.5$.

the sensor, i.e., $R_s = (1 + \tau)|-R|$ and $(\tau \ll 1)$, the eigenfrequencies of the third-order *PT/PTX* system can be approximately expressed as follows:

$$\omega_{1}' \approx \omega_{0} \sqrt{\frac{2\gamma^{2} - 1 - \tau - \sqrt{(1+\tau)^{2} - 4\gamma^{2}(1+\tau) + 8\gamma^{4}\kappa^{2}}}{2\gamma^{2}(1-2\kappa^{2})}}$$
(3a)

$$\omega_2' \approx \omega_0 \left(= 1/\sqrt{LC} \right)$$
 (3b)

$$\omega_{3}' \approx \omega_{0} \sqrt{\frac{2\gamma^{2} - 1 - \tau + \sqrt{(1+\tau)^{2} - 4\gamma^{2}(1+\tau) + 8\gamma^{4}\kappa^{2}}}{2\gamma^{2}(1-2\kappa^{2})}}.$$
(3c)

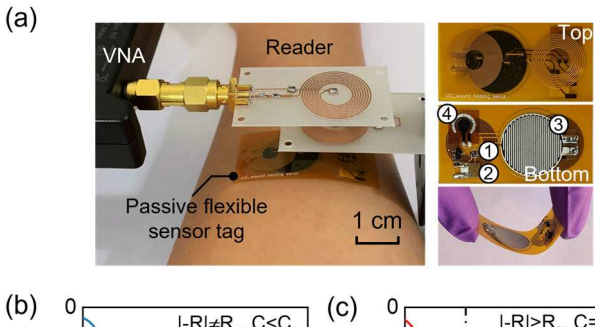
We note that in case $\tau=0$, which conveys that the system satisfies the PT/PTX symmetry, (3) is equivalent to (1). Equation (3) states that with slightly unbalanced resistance in the sensor and reader, ω_1 and ω_3 are influenced by the resistive perturbation while ω_2 remains unchanged. Therefore, we conclude that whether the system is symmetric or slightly asymmetric in resistance, ω_2 is only related to L and C values and is independent of γ and κ .

Since the coil inductance L and coupling coefficient κ are fixed, the equivalent capacitance C can be determined from the offset of ω_2 . After the equivalent capacitance of the sensor is obtained, the effective resistance of the sensor can be obtained by tracking ω_1 or ω_3 , which varies with $\gamma = R^{-1}\sqrt{L/C}$.

One can first adjust the varactors on both the reader and intermediator to attain a distinct resonance at ω_2 . Subsequently, by fine-tuning the effective resistance of the reader, three resonant dips can be observed in the reflection spectrum (i.e., the exact PT symmetry). This step enables retrieving the sensor's resistance R. As a consequence, the third-order PTsymmetric sensing system allows for simultaneously detecting resistive and capacitive changes on the sensor, which may not be possible with standard second-order PT-symmetric system [23], [29], [37] or traditional passive wireless sensing methods [21], [44], [45]. In the pursuit of optimal wound management, we utilize the third-order *PT/PTX*-symmetric system with two tank sensors, as shown in Fig. 1(b), for simultaneous monitoring of multiple biomarkers crucial to the healing process. This approach allows us to precisely track two resistive parameters, namely, temperature and pressure, along with two capacitive parameters, humidity and pH. It is worth highlighting that through judicious adaptations of the sensors and transducers, the PT/PTX telemetry platform may also facilitate concurrent detection of other wound site parameters and biological indicators, including but not limited to oxygen, thermal conductivity, and uric acid.

III. EXPERIMENTAL DEMONSTRATION

Fig. 3(a) shows the photograph of the PT/PTX sensing platform (left) and the flexible, wearable wound sensor embedded in a smart bandage (right). When monitoring wound status, the smart bandage can be easily affixed onto the wound site, while the associated reader is directly connected to a vector network analyzer (VNA) to acquire the reflection spectrum. As shown in Fig. 3(a), the *PT/PTX*-symmetric wound sensor consists of: 1) a negative temperature coefficient (NTC) thermistor from Murata Electronics (NCP15XC680E03RC); 2) a capacitive humidity sensor from Innovative Sensor Technology (P14-W); 3) a force sensing resistor from Ohmite (FSR06BE); and 4) a custom-made pH sensor, fabricated by polyaniline modification of laser-induced graphene electrodes. The integrated smart bandage is based on a single flexible polyimide substrate with a thickness of only 0.16 mm, rendering it eminently suited for deployment in wearable technology. The wound parameters to be monitored can be derived from the resonance dips in the measured reflection spectrum, provided that the coil inductance L and coupling strength κ are fixed at appropriate values. As shown in Fig. 3(b), a reflection minimum was first found at f_2 by tuning the capacitance of the intermediator and reader, and the resonance frequency f_2 is used as a sign of balance in capacitance (i.e., $C = C_s$); here, the three resonant frequencies are denoted by $f_n = \omega_n/2\pi$, n = 1, 2, and 3. Three reflection dips were then acquired by adjusting the resistance of the reader until the PT symmetry is achieved (i.e., $|-R| = R_s$, $C = C_s$) [Fig. 3(c)]. By this simple, two-step tracking of resonance frequencies of the third-order PT/PTXsymmetric system, R_s and C_s values can be obtained with high accuracy. It is evidently seen from Fig. 3(c) that resonance at f_2 is dominated by the capacitance of the system and is unaffected if the resistance values of the reader and the sensor are slightly different. What observed from Fig. 3(b) and (c) is consistent with the theoretical result in (3), indicating that



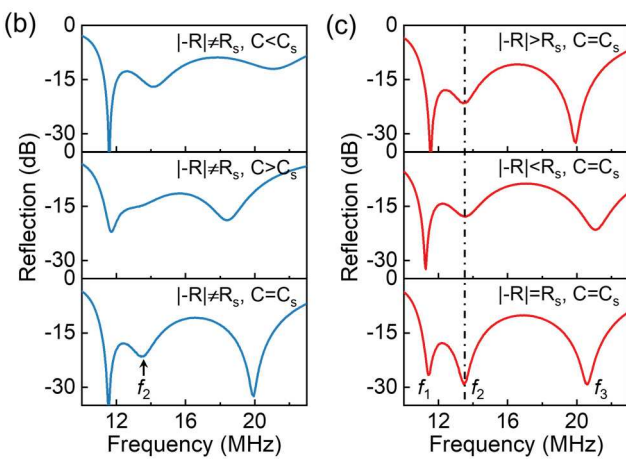


Fig. 3. (a) Photograph of experimental setup for the wound monitoring system (left) and the compact, flexible, and wearable wound sensor (right). Measured reflection spectra for two scenarios: (b) when both R_s and C_s are unknown, one first tries to determine C_s , and (c) after C_s is known, one tries to find the exact value of R_s .

the proposed sensing mechanism can be effective for multiplexed sensing of the wound site. During the experiment, the coupling coefficient κ , associated with the distance between the neighboring coils, was kept at a fixed value of 0.45. The value of κ is chosen to make the system operate close to the EP.

A. Temperature and Humidity Monitoring

During the measurement of temperature and humidity, the coil inductance L is fixed at 1120 nH, and the equivalent resistance and capacitance of the sensor are influenced by temperature and RH, respectively. The NTC thermistor, with a parallel connected resistor of 182 Ω , exhibits an equivalent resistance of 48.7 Ω at room temperature (25 °C). The capacitance of the capacitive humidity sensor is measured to be 126.6 pF at 30% RH, such that at 25 °C and 30% RH, $\gamma = 1.93$ and the system operates around the EP. Fig. 4(a) shows the reflection spectra of the wound sensing system under different temperature conditions; here, RH = 30%. The experimental results (solid lines) show great consistency with theoretical ones (dashed lines). It is observed from Fig. 4(a) that f_1 and f_3 respond sensitively to temperature variations, while f_2 remains constant. This agrees with the previous theoretical investigation that f_2 is only affected by the sensor's effective capacitance related to RH. We note that while both f_1 and f_3 are responsive to variations in temperature, the latter one shows a more remarkable shift due to the eigenfrequency bifurcation effect discussed in the previous section (Fig. 2).

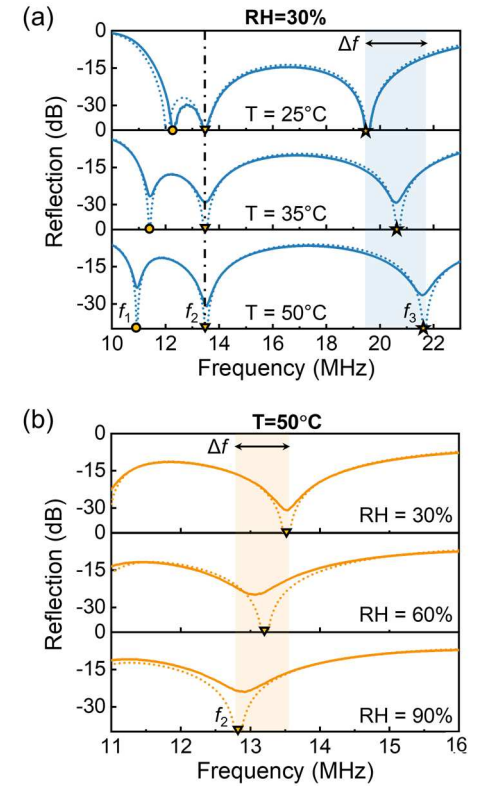


Fig. 4. Reflection spectra of the PT/PTX-symmetric wound monitoring system with (a) 30% RH and different temperature and (b) 50 °C and different RH. Here, the solid and dashed lines, respectively, represent the measured and calculated results.

Therefore, the detection of wound temperature is undertaken by tracing the shifts of the third resonant frequency f_3 or the frequency ratio f_3/f_2 . Fig. 4(b) plots the resonance at f_2 with different RHs, which further demonstrates the feasibility of monitoring RH levels through the detection of shifts in the resonant frequency f_2 .

The influence of RH on the capacitance of the humidity sensor is presented in Fig. 5(a), where a notable increase from 126.6 to 138.1 pF is observed upon an increase in RH from 30% to 90%. The increase in capacitance results in a downshifting f_2 . The frequency shift Δf_2 as a function of RH is shown in Fig. 5(b); here, $\Delta f_2 = f_2 - f_2|_{\text{RH}=90\%}$. As RH ascends from 30% to 90%, the increase in capacitance leads to a drop of f_2 by approximately 600 kHz, indicating a sensitivity of 9.3 kHz/%RH. Fig. 5(c) depicts the variation in the equivalent resistance of the NTC thermistor, which is proportional to temperature changes. We find that the equivalent resistance decreases from 48.7 to 26.6 Ω , as temperature increases from 25 °C to 50 °C. The reduction in resistance increases the value of γ , and thus, the frequency ratio f_3/f_2 increases with temperature, as presented in Fig. 5(d). When the RH is 30% and 90%, the sensitivity of monitoring temperature is 81.1 kHz/°C and 84.7 kHz/°C, respectively. Sensitivity increases slightly with the moisture level, as higher RH corresponds to a higher capacitance and thus a lower gain-loss parameter γ (closer to γ_{EP}). The sensing ranges (i.e., 25 °C– 50 °C and 30%–90% RH) may cover all possible variations in

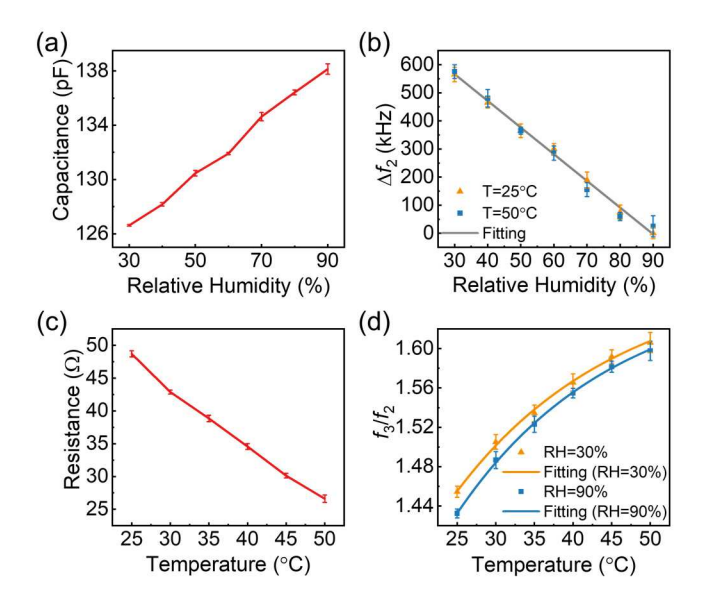
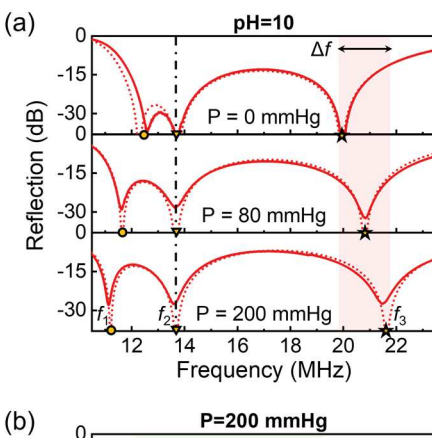


Fig. 5. (a) Measured capacitance of the capacitive humidity sensor versus RH. (b) Frequency shift Δf_2 as a function of RH. (c) Measured equivalent resistance of the NTC thermistor versus temperature. (d) Frequency ratio f_3/f_2 as a function of temperature. The error bars are generated from three measurements.

temperature and humidity around the wound site. It is evident from Fig. 5(b) and (d) that the relationship between Δf_2 and RH remains constant irrespective of temperature. Furthermore, once RH is ascertained, the relationship between f_3/f_2 and temperature becomes apparent [Equation (1c)]. Therefore, the third-order *PT/PTX*-symmetric sensor possesses the capability to simultaneously acquire wound temperature and humidity. Moreover, the sensitivity levels for both temperature and humidity sensing are highly commendable. In particular, the sensitivity of resistive temperature sensing experiences a considerable enhancement due to the eigenfrequency bifurcation occurring around the EP and can be further improved when the system is operated near the divergent EP (DEP) [22], [24], [25]. In addition, there are several deficiencies in experimental measurements, including asymmetric coupling, fabrication errors, and parasitic effects of the circuit boards, which slightly destroy the PT-symmetric condition and could affect the accuracy of the measurement results. The performance of the PT-symmetric wound sensor may be further improved through several strategies. For instance, a feedback control system could be utilized to precisely pitch the positions of the reader and intermediator, ensuring consistency of the coupling strength between the reader and intermediator and that between the intermediator and sensor. A properly designed dielectric spacer made of low-permittivity materials can also provide better coil alignment. In addition, the errors due to parasitic effects and manufacturing flaws can be significantly suppressed by using the advanced complementary metal-oxide semiconductor (CMOS) integrated circuit and packaging technology (e.g., on-chip RF reader).

B. Pressure and pH Monitoring

To obtain pressure and pH around the wound, the reader and intermediator used are the same as those used in temperature



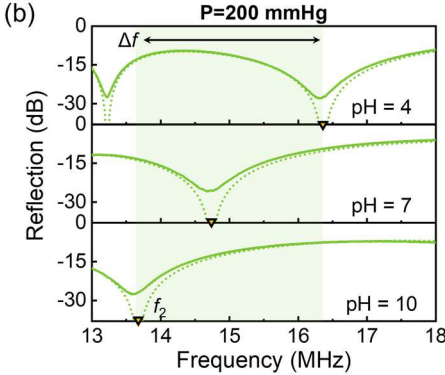


Fig. 6. Reflection spectra of the PT/PTX-symmetric wound monitoring system with (a) pH = 10 and different pressures and (b) P = 200 mmHg and different pH values. Here, the solid and dashed lines, respectively, represent the measured and calculated results.

and humidity monitoring, namely, that their coil inductance is still 1120 nH. The passive RLC tank sensor follows the reciprocal scaling rule, where the scaling factor x = 3.8. Here, the variations in resistance and capacitance, respectively, correspond to the changes in pressure and pH. The force sensing resistor (in parallel with a 187- Ω resistor to fulfill PTX-symmetric condition) has an equivalent resistance of \sim 187 Ω at 0 mmHg. The pH sensor is connected in parallel with a voltage-controlled varactor diode (MAVR-000405-0287FT, MACOM Technology Solutions). Thus, the changes in the potential difference between pH electrodes (i.e., a reference electrode, RE, and a sensing electrode, SE) can be translated to capacitance variations. At pH = 10, the equivalent capacitance of the sensor is measured to be 31.8 pF. The gain-loss parameter γ is thus 1.96 at 0 mmHg and 10 pH. Fig. 6(a) and (b) plots the reflection coefficients with different pressures and pH, respectively, where the solid (dashed) lines denote the measured (calculated) results. As with our prior analysis, the pressure that corresponds to the resistance value can be monitored by tracking the alteration in the third resonant frequency f_3 or the frequency ratio f_3/f_2 , and the pH level that corresponds to the capacitance value can be obtained directly from the second resonant frequency f_2 .

Fig. 7(a) presents the measured electrode potential and capacitance at different pH levels. The electrode potential, which serves as the bias voltage for the varactor diode, decreases with increasing pH. As pH increases from 4 to 10,

an increase in the capacitance from 22.5 to 31.8 pF can be observed, giving rise to a left shift of f_2 . Fig. 7(b) illustrates the frequency drift Δf_2 ($\Delta f_2 = f_2 - f_2|_{\text{pH}=10}$) with different pH levels, showing a ~2500-kHz frequency change when pH varies from 4 to 10. It is seen that the pH can be read from f_2 regardless of the pressure conditions. The sensitivity of monitoring pH remains at 434.0 kHz per unit change in pH. After the pH level is acquired, a direct correspondence can be found between the pressure and the frequency ratio f_3/f_2 . Fig. 7(c) shows the equivalent resistance of the force-sensing resistor as a function of pressure. We see that its equivalent resistance is \sim 187 Ω at 0 mmHg, and as pressure increases to 200 mmHg, the resistance drops to \sim 120 Ω . With pressure increases, the resistance drop results in an increase in the gain-loss parameter γ and also an increase in f_3/f_2 , as described in Fig. 7(d). The sensitivity of pressure monitoring, calculated as the shift of f_3 , is 6.4 kHz/mmHg when pH = 4 and is 7.8 kHz/mmHg when pH = 10. Again, the sensitivity slightly increases with pH, as higher pH pushes the system closer to the EP. By virtue of the proposed PT/PTX-symmetric sensing platform, the pressure and pH are simultaneously detected with excellent linearity and sensitivity. The sensing performance of the PT/PTX-symmetric wound sensor could be further improved by using a set of γ and κ closer to the EP or DEP and reducing the parasitic effects and losses in the circuit components. The wound parameters monitored in this work (i.e., temperature, humidity, pressure, and pH) play an important role in assessing the wound healing process. Besides these, the PT/PTX sensing system may also be applied to detect other clinically significant biomarkers, such as strain, uric acid, and oxygen concentration. We envision that the proposed PT/PTX-symmetric sensing system would serve as a steppingstone toward chronic wound management, wearable biotelemetry, as well as various noninvasive techniques.

C. In Vitro Demonstration

To further validate the wound healing sensing system, a series of in vitro experiments are conducted. Specifically, the performance of the wound sensor is compared when the sensor tag is placed in the air, affixed to human skin, and affixed to a fish. As clearly illustrated in Fig. 8(a) and (b), the ultrathin and flexible characteristics of the wound sensor afford it the ability to conform seamlessly to the curved surfaces of human skin and piscine organisms. Fig. 8(c) displays the reflection spectrum of the system under identical temperature and RH conditions, with the sensor tag positioned in three different settings, namely, in the air, on human skin, and on a fish. The temperature employed in this investigation is 33.2 °C, corresponding to the typical skin temperature. To ensure uniformity in temperature conditions, a hotplate is employed to sustain a temperature of 33.2 °C for the sensor tag located in the air and affixed to the fish, which closely approximates the temperature of human skin. Furthermore, the ambient RH is consistently maintained at a level of 30%. As seen in Fig. 8(c), despite the tag being placed on different substrates (air, human, and fish), the measured reflection spectra are nearly the same as long

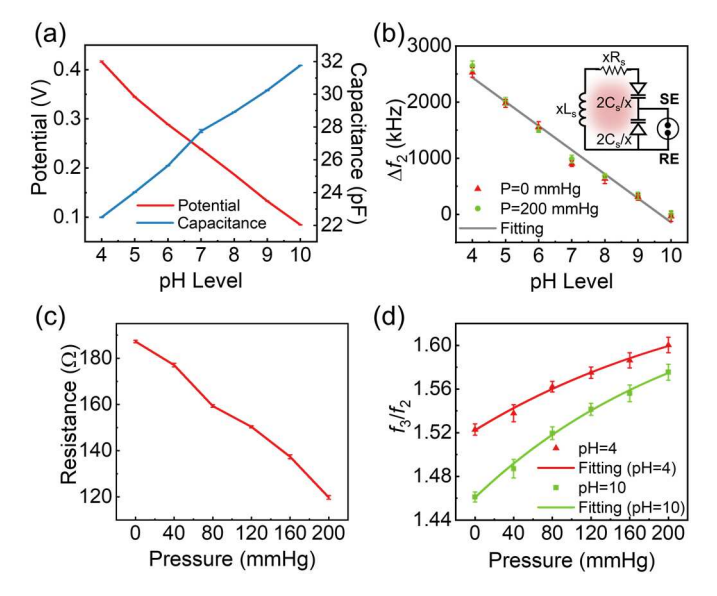


Fig. 7. (a) Potential difference between the pH electrodes (left axis) and equivalent capacitance of the sensor (right axis) versus pH level. (b) Frequency shift Δf_2 as a function of pH level. Inset: schematic of the tank sensor when performing pressure and pH measurement. (c) Equivalent resistance of the force sensing resistor versus pressure. (d) Frequency ratio f_3/f_2 as a function of pressure. The error bars are generated from three measurements.

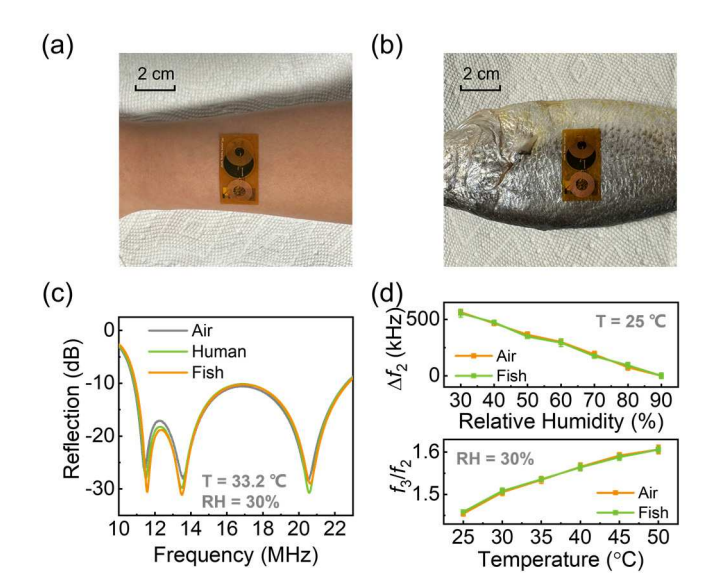


Fig. 8. Photographs of the wound sensor (a) affixed to human skin and (b) affixed to a fish. The reader setup is exactly the same as that shown in Fig. 3(a). (c) Measured reflection spectrum of the wound sensing system with T = 33.2 °C and RH = 30%. (d) Frequency shift Δf_2 as a function of RH with T = 25 °C (top). Frequency ratio f_3/f_2 as a function of temperature with RH = 30% (bottom). (c) and (d) Indicate that the resonant frequency and sensing efficacy of the wound sensor exhibit remarkable consistency when deployed in air, adhered to human skin, and adhered to a fish.

as the same temperature and RH are ensured. The resonant frequencies, or resonant dips, which encode the information of sensing parameters, are barely affected by the presence of the human body or animal tissue. This is due to the fact that the communication between the reader and sensor tag is through inductive links. The coupling strength between coil

inductors is unrelated to the permittivity but only related to the permeability of the dielectric media. For most dielectric media, including biological tissues and liquids, the permeability has a constant value of 1. Consequently, the presence of human, fish, or other biological tissues has little impact on the inductive coupling strength and resonant frequency of the wound sensing system.

Fig. 8(d) compares the performance of the wound sensor when used to monitor RH (top; temperature is fixed at 25 °C) and temperature (bottom; RH is fixed at 30%). It can be seen that the frequency shift Δf_2 as a function of RH and the ratio f_3/f_2 as a function of temperature are almost unaffected whether the tag is placed in the air or affixed to a fish. Our in vitro experiments demonstrate that the proposed wound monitoring system performs with good consistency and reliability, even in the presence of biological tissues. These findings underscore the sensor's potential as an appealing solution for wound monitoring and diverse wearable medical and health monitoring applications.

IV. CONCLUSION

We have proposed the multifunctional PT/PTX-symmetric sensing platform with great potential for applications in real-time wireless wound monitoring and management. We have theoretically studied and practically implemented the proposed sensing platform, which enables simultaneous monitoring of multiple physiological parameters associated with capacitive and resistive perturbations on the sensor. Specifically, we have experimentally demonstrated the simultaneous in situ detection of body temperature, RH, pressure, and pH, which are all relevant indicators of wound status. In addition, we have performed in vitro tests to verify and validate that the effectiveness, uniformity, and reliability of the proposed wireless wound monitoring technique when the compact wearable sensor is in contact with the human skin and animal tissue. Such a fully passive and wireless multiplex sensing platform may be beneficial for developing the next-generation wearable biomedical devices and systems.

REFERENCES

- [1] N. S. Oliver, C. Toumazou, A. E. G. Cass, and D. G. Johnston, "Glucose sensors: A review of current and emerging technology," *Diabetic Med.*, vol. 26, no. 3, pp. 197–210, Mar. 2009, doi: 10.1111/j.1464-5491.2008.02642.x.
- [2] H. Fassbender et al., "Fully implantable blood pressure sensor for hypertonic patients," in *Proc. IEEE Sensors*, Oct. 2008, pp. 1226–1229, doi: 10.1109/icsens.2008.4716664.
- [3] B. Yu, L. Xu, and Y. Li, "Bluetooth low energy (BLE) based mobile electrocardiogram monitoring system," in *Proc. IEEE Int. Conf. Inf. Autom.*, Jun. 2012, pp. 763–767, doi: 10.1109/ICInfA.2012.6246921.
- [4] K. Zheng, S. Chen, L. Zhu, J. Zhao, and X. Guo, "Large area solution processed poly (Dimethylsiloxane)-based thin film sensor patch for wearable electrocardiogram detection," *IEEE Elec*tron Device Lett., vol. 39, no. 3, pp. 424–427, Mar. 2018, doi: 10.1109/LED.2018.2792022.
- [5] Z. Ye et al., "A breathable, reusable, and zero-power smart face mask for wireless cough and mask-wearing monitoring," ACS Nano, vol. 16, no. 4, pp. 5874–5884, Apr. 2022, doi: 10.1021/acsnano.1c11041.
- [6] M. Olsson et al., "The humanistic and economic burden of chronic wounds: A systematic review," Wound Repair Regener., vol. 27, no. 1, pp. 114–125, Jan. 2019, doi: 10.1111/wrr.12683.

- [7] H. Derakhshandeh, S. S. Kashaf, F. Aghabaglou, I. O. Ghanavati, and A. Tamayol, "Smart bandages: The future of wound care," *Trends Biotechnol.*, vol. 36, no. 12, pp. 1259–1274, Dec. 2018, doi: 10.1016/j.tibtech.2018.07.007.
- [8] J. G. Powers, C. Higham, K. Broussard, and T. J. Phillips, "Wound healing and treating wounds," *J. Amer. Acad. Dermatol.*, vol. 74, no. 4, pp. 607–625, Apr. 2016, doi: 10.1016/j.jaad.2015.08.070.
- [9] R. Lim, D. S. W. Choong, and M.-Y. Cheng, "Development of integrated pressure and temperature sensing strips for monitoring venous leg ulcer application," in *Proc. IEEE 70th Electron. Compon. Technol. Conf. (ECTC)*, Jun. 2020, pp. 1586–1591, doi: 10.1109/ECTC32862.2020.00249.
- [10] N. Tang et al., "Wearable sensors and systems for wound healing-related pH and temperature detection," *Micromachines*, vol. 12, no. 4, p. 430, Apr. 2021, doi: 10.3390/mi12040430.
- [11] S.-H. Lu et al., "Multimodal sensing and therapeutic systems for wound healing and management: A review," Sens. Actuators Rep., vol. 4, Nov. 2022, Art. no. 100075, doi: 10.1016/j.snr.2022.100075.
- [12] D. Gomez, S. P. Morgan, B. R. H. Gill, and S. Korposh, "Polymeric fibre optic sensor based on a SiO₂ nanoparticle film for humidity sensing on wounds," *Proc. SPIE*, vol. 9916, pp. 294–297, May 2016, doi: 10.1117/12.2236845.
- [13] P. Kassal et al., "Smart bandage with wireless connectivity for uric acid biosensing as an indicator of wound status," *Electrochemistry Commun.*, vol. 56, pp. 6–10, Jul. 2015, doi: 10.1016/j.elecom.2015. 03.018.
- [14] R. Rahimi et al., "A low-cost flexible pH sensor array for wound assessment," Sens. Actuators B, Chem., vol. 229, pp. 609–617, Jun. 2016, doi: 10.1016/j.snb.2015.12.082.
- [15] M. Ochoa et al., "Integrated sensing and delivery of oxygen for next-generation smart wound dressings," *Microsyst. Nanoeng.*, vol. 6, no. 1, p. 46, May 2020, doi: 10.1038/s41378-020-0141-7.
- [16] M. F. Farooqui and A. Shamim, "Low cost inkjet printed smart bandage for wireless monitoring of chronic wounds," *Sci. Rep.*, vol. 6, no. 1, p. 28949, Jun. 2016, doi: 10.1038/srep28949.
- [17] M. Jose et al., "Stretchable printed device for the simultaneous sensing of temperature and strain validated in a mouse wound healing model," *Sci. Rep.*, vol. 12, no. 1, p. 10138, Jun. 2022, doi: 10.1038/s41598-022-13834-6.
- [18] Y. Hattori et al., "Multifunctional skin-like electronics for quantitative, clinical monitoring of cutaneous wound healing," Adv. Healthcare Mater., vol. 3, no. 10, pp. 1597–1607, Oct. 2014, doi: 10.1002/adhm.201400073.
- [19] A. Tamayol et al., "Flexible pH-sensing hydrogel fibers for epidermal applications," Adv. Healthcare Mater., vol. 5, no. 6, pp. 711–719, Mar. 2016, doi: 10.1002/adhm.201500553.
- [20] T. Guinovart, G. Valdés-Ramírez, J. R. Windmiller, F. J. Andrade, and J. Wang, "Bandage-based wearable potentiometric sensor for monitoring wound pH," *Electroanalysis*, vol. 26, no. 6, pp. 1345–1353, Jun. 2014, doi: 10.1002/elan.201300558.
- [21] W.-J. Deng, L.-F. Wang, L. Dong, and Q.-A. Huang, "LC wireless sensitive pressure sensors with microstructured PDMS dielectric layers for wound monitoring," *IEEE Sensors J.*, vol. 18, no. 12, pp. 4886–4892, Jun. 2018, doi: 10.1109/JSEN.2018.2831229.
- [22] M. Sakhdari, Z. Ye, M. Farhat, and P.-Y. Chen, "Generalized theory of PT-symmetric radio-frequency systems with divergent exceptional points," *IEEE Trans. Antennas Propag.*, vol. 70, no. 10, pp. 9396–9405, Oct. 2022, doi: 10.1109/TAP.2022.3179528.
- [23] P.-Y. Chen et al., "Generalized parity-time symmetry condition for enhanced sensor telemetry," *Nature Electron.*, vol. 1, no. 5, pp. 297–304, May 2018, doi: 10.1038/s41928-018-0072-6.
- [24] M. Sakhdari, M. Hajizadegan, Q. Zhong, D. N. Christodoulides, R. El-Ganainy, and P.-Y. Chen, "Experimental observation of PT symmetry breaking near divergent exceptional points," *Phys. Rev. Lett.*, vol. 123, no. 19, Nov. 2019, Art. no. 193901, doi: 10.1103/Phys-RevLett.123.193901.
- [25] M. Sakhdari, M. Hajizadegan, and P. Y. Chen, "Robust extended-range wireless power transfer using a higher-order PT-symmetric platform," *Phys. Rev. Res.*, vol. 2, Feb. 2020, Art. no. 013152, doi: 10.1103/Phys-RevResearch.2.013152.
- [26] Y.-H. Lin, Y.-C. Chen, K.-S. Cheng, P.-J. Yu, J.-L. Wang, and N.-Y. Ko, "Higher periwound temperature associated with wound healing of pressure ulcers detected by infrared thermography," *J. Clin. Med.*, vol. 10, no. 13, p. 2883, Jun. 2021, doi: 10.3390/jcm10132883.

- [27] M. Fierheller and R. G. Sibbald, "A clinical investigation into the relationship between increased periwound skin temperature and local wound infection in patients with chronic leg ulcers," Adv. Skin Wound Care, vol. 23, no. 8, pp. 369–379, Aug. 2010, doi: 10.1097/01.asw.0000383197.28192.98.
- [28] D. Okan, K. Woo, E. A. Ayello, and G. Sibbald, "The role of moisture balance in wound healing," Adv. Skin Wound Care, vol. 20, no. 1, pp. 54–55, Jan. 2007.
- [29] M. Sakhdari, M. Hajizadegan, Y. Li, M. M. Cheng, J. C. H. Hung, and P.-Y. Chen, "Ultrasensitive, parity-time-symmetric wireless reactive and resistive sensors," *IEEE Sensors J.*, vol. 18, no. 23, pp. 9548–9555, Dec. 2018, doi: 10.1109/JSEN.2018.2870322.
- [30] M.-Y. Yang, Z.-L. Ye, L. Zhu, M. Farhat, and P.-Y. Chen, "Recent advances in coherent perfect absorber-lasers and their future applications," *J. Central South Univ.*, vol. 29, no. 10, pp. 3203–3216, Oct. 2022, doi: 10.1007/s11771-022-5160-0.
- [31] M. Yang, Z. Ye, M. Farhat, and P.-Y. Chen, "Enhanced radio-frequency sensors based on a self-dual emitter-absorber," *Phys. Rev. Appl.*, vol. 15, no. 1, Jan. 2021, Art. no. 014026, doi: 10.1103/physrevapplied.15.014026.
- [32] M. Yang, Z. Ye, and P.-Y. Chen, "A quantum-inspired biotelemetry system for robust and ultrasensitive wireless intracranial pressure monitoring," in *Proc. IEEE Sensors*, Oct. 2021, pp. 1–4, doi: 10.1109/SEN-SORS47087.2021.9639684.
- [33] Z. Ye, M. Yang, and P.-Y. Chen, "Multi-band parity-time-symmetric wireless power transfer systems for ISM-band bio-implantable applications," *IEEE J. Electromagn., RF Microw. Med. Biol.*, vol. 6, no. 2, pp. 196–203, Jun. 2022, doi: 10.1109/JERM.2021.3120621.
- [34] R. El-Ganainy, K. G. Makris, D. N. Christodoulides, and Z. H. Musslimani, "Theory of coupled optical PT-symmetric structures," Opt. Lett., vol. 32, no. 17, p. 2632, Sep. 2007, doi: 10.1364/ol.32.002632.
- [35] M.-A. Miri and A. Alu, "Exceptional points in optics and photonics," Science, vol. 363, Jan. 2019, Art. no. eaar7709, doi: 10.1126/science.aar7709.
- [36] M. Yang, Z. Ye, M. Farhat, and P.-Y. Chen, "Ultrarobust wireless interrogation for sensors and transducers: A non-hermitian telemetry technique," *IEEE Trans. Instrum. Meas.*, vol. 70, pp. 1–9, 2021, doi: 10.1109/TIM.2021.3107057.
- [37] M. Yang, Z. Ye, N. Alsaab, M. Farhat, and P.-Y. Chen, "In-vitro demonstration of ultra-reliable, wireless and batteryless implanted intracranial sensors operated on loci of exceptional points," *IEEE Trans. Biomed. Circuits Syst.*, vol. 16, no. 2, pp. 287–295, Apr. 2022, doi: 10.1109/TBCAS.2022.3164697.
- [38] M. Farhat, M. Yang, Z. Ye, and P.-Y. Chen, "PT-symmetric absorber-laser enables electromagnetic sensors with unprecedented sensitivity," ACS Photon., vol. 7, no. 8, pp. 2080–2088, Aug. 2020, doi: 10.1021/acsphotonics.0c00514.
- [39] Z. Ye, M. Yang, L. Zhu, and P.-Y. Chen, "PTX-symmetric metasurfaces for sensing applications," *Frontiers Optoelectronics*, vol. 14, no. 2, pp. 211–220, Jun. 2021, doi: 10.1007/s12200-021-1204-6.
- [40] M. Yang, Z. Ye, M. Farhat, and P.-Y. Chen, "Cascaded PT-symmetric artificial sheets: Multimodal manipulation of self-dual emitter-absorber singularities, and unidirectional and bidirectional reflectionless transparencies," *J. Phys. D, Appl. Phys.*, vol. 55, no. 8, Nov. 2021, Art. no. 085301, doi: 10.1088/1361-6463/ac3300.
- [41] Z. Ye, M. Yang, and P. Y. Chen, "Metasurface absorber-emitter for humidity sensing," URSI Radio Sci. Lett., vol. 3, pp. 1–5, 2021, doi: 10.46620/21-0029.
- [42] R. Fleury, D. Sounas, and A. Alu, "An invisible acoustic sensor based on parity-time symmetry," *Nature Commun.*, vol. 6, no. 1, p. 5905, Jan. 2015, doi: 10.1038/ncomms6905.
- [43] Z. Ye, M. Farhat, and P.-Y. Chen, "Tunability and switching of Fano and Lorentz resonances in PTX-symmetric electronic systems," *Appl. Phys. Lett.*, vol. 117, no. 3, Jul. 2020, Art. no. 031101, doi: 10.1063/5.0014919.
- [44] P.-J. Chen, S. Saati, R. Varma, M. S. Humayun, and Y.-C. Tai, "Wireless intraocular pressure sensing using microfabricated minimally invasive flexible-coiled LC sensor implant," *J. Microelectromech. Syst.*, vol. 19, no. 4, pp. 721–734, Aug. 2010, doi: 10.1109/JMEMS.2010.2049825.
- [45] Q.-A. Huang, L. Dong, and L.-F. Wang, "LC passive wireless sensors toward a wireless sensing platform: Status, prospects, and challenges," *J. Microelectromech. Syst.*, vol. 25, no. 5, pp. 822–841, Oct. 2016, doi: 10.1109/JMEMS.2016.2602298.

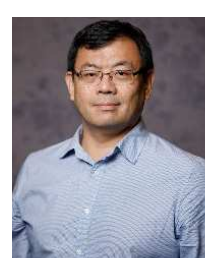


Zhilu Ye received the B.S. degree in microelectronics from the Huazhong University of Science and Technology, Wuhan, China, in 2018, the master's degree in electrical engineering from Arizona State University, Tempe, AZ, USA, in 2019, and the Ph.D. degree from the University of Illinois at Chicago, Chicago, IL, USA, in 2023.

Since then, she has been serving as an Assistant Professor with the School of Life Science and Technology, Xi'an Jiaotong University, Xi'an,

China. Her research areas include applied electromagnetics, antennas, radio frequency and microwave circuits, and their applications in wireless biomedical sensors, wearable and implantable devices, telemedicine, and healthcare Internet of Things.

Dr. Ye was granted the 2022 Dean's Scholar Fellowship from the University of Illinois at Chicago, the USNC-URSI 2022 Travel Fellowship from the National Academy of Sciences, the nomination for the IEEE Sensors 2022 Best Paper Award, and the second place for the IEEE AP-S/URSI 2022 Student Design Contest.



Mark M.-C. Cheng (Senior Member, IEEE) received the B.S. and Ph.D. degrees from National Tsing-Hua University, Hsinchu, Taiwan, in 1995 and 2003, respectively.

He was a Research Assistant Professor with the Department of Nanomedicine and Biomedical Engineering, University of Texas Health Science Center at Houston, Houston, TX, USA, from 2006 to 2007. In 2008, he joined Wayne State University (WSU), Detroit, MI, USA, where he became a Full Professor in 2019. At WSU,

he initialized curriculum in Nanoengineering and Cyber-Physical Systems (CPS). In 2019, he joined the Department of electrical and Computer Engineering, University of Alabama, Tuscaloosa, AL, USA, where he is currently a Professor. He has authored approximately 120 articles in peer-reviewed journal and conference proceedings. He has been involved in multidisciplinary research in microsystem design, biomedical devices, biosensor, new materials, wearable sensors, and environmental Interne of Things (IoT).

Dr. Cheng was a recipient of the National Science (NSF) CAREER Award, the ONR Summer Faculty Fellowship, and the President Research Enhancement Award.



Minye Yang received the bachelor's degree in optical and electronic information from the Huazhong University of Science and Technology, Wuhan, China, in 2018, the M.Sc. degree in electrical engineering from Wayne State University, Detroit, MI, USA, in 2019, and the Ph.D. degree from the University of Illinois Chicago, Chicago, IL, USA, in 2023.

He is now serving as an Assistant Professor with the School of Electronics Science and Technology, Xi'an Jiaotong University, Xi'an, China.

His research mainly focuses on applied electromagnetics, including non-Hermitian physics, ultrasensitive sensors, radio frequency/microwave circuits, noninvasive biomedical sensing, soft/wearable electronics, and electromagnetically enabled hardware securities.

Dr. Yang was a recipient of the 2022 URSI-NRSM Travel Grant and the Nomination for the Best Paper Award of IEEE Sensors in 2022. He was awarded the Young Talented Scientist by Xi'an Jiaotong University.



Pai-Yen Chen (Senior Member, IEEE) received the B.S. and M.S. degrees from National Chiao Tung University, Hsinchu, Taiwan, in 2004 and 2006, respectively, and the Ph.D. degree from the University of Texas at Austin, Austin, TX, USA, in 2013.

He was an Assistant Professor with Wayne State University (WSU), Detroit, MI, USA, from 2014 to 2018, and a Research Scientist with Intellectual Ventures' Metamaterial Commercialization Center, Bellevue, WA, USA.

from 2013 to 2014, and a Research Staff with the Taiwan Semiconductor Research Institute (TSRI), Hsinchu, from 2006 to 2009. He is an Associate Professor with the Department of Electrical and Computer Engineering, University of Illinois at Chicago (UIC), Chicago, IL, USA. He has been involved in multidisciplinary research on applied electromagnetics, RF and microwave antennas and circuits, metamaterials, metasurfaces, wireless sensors and systems, nanoelectromagnetism, plasmonics, nanophotonics, and nanoelectronics.

Dr. Chen has received quite a few prestigious awards, including National Science Foundation (NSF) CAREER Award, the IEEE Sensors Council Young Professional Award, the IEEE Raj Mittra Travel Grant (RMTG) Award, the Society of Photo-Optical Instrumentation Engineers (SPIE) Rising Researcher Award, the Applied Computational Electromagnetics Society (ACES) Early Career Award, the Photonics and Electromagnetics Research Symposium (PIERS) Young Scientist Award, the Young Scientist Awards from Union Radio-Scientifique Internationale (URSI) General Assembly and URSI Commission B: Electromagnetics, Institute of Physics (IOP) Measurement Science and Technology Emerging Leader, the Air Force Research Laboratory Faculty Fellowship, the UIC College of Engineering Faculty Research Award, the WSU College of Engineering Faculty Research Excellence Award, the Donald Harrington Fellowship, Taiwan Ministry of Education Study Abroad Award, the United Microelectronics Corporation Scholarship, and quite a few best paper awards and travel grants from major IEEE conferences, including IEEE Antennas and Propagation Symposium in 2011, 2013, 2016, and 2021, the IEEE International Microwave Symposium in 2015, the IEEE Sensors Conference in 2016, the IEEE Wireless Power Transfer Conference in 2021, and the USNC-URSI Ernest K. Smith Student Paper Award in 2012. He currently serves as an Associate Editor for IEEE Sensors Journal, IEEE TRANSACTIONS ON ANTENNAS AND PROPAGATION, and IEEE Antennas and Wireless Propagation Letters, and a Lead Guest Editor for IEEE Journal of Selected Areas in Sensors. He was a Former Associate Editor of Applied Electromagnetics, IEEE Journal of Radio Frequency Identification, and IEEE Journal of Electromagnetics, RF and Microwaves in Medicine and Biology (IEEE-JERM), and a Former Guest Editor of the IEEE TRANSACTIONS ON ANTENNAS AND PROPAGATION.



Mohamed Farhat received the master's degree in theoretical physics and the Ph.D. degree in optics and electromagnetism from Aix-Marseille University, Aix-en-Provence, France, in 2006 and 2010, respectively.

His Ph.D. dissertation was titled by "Metamaterials for Harmonic and Biharmonic Cloaking and Superlensing." He has authored more than 100 publications, including one edited book, 94 journal papers, seven book chapters, and five international patents, as well as more than

90 conference papers, with more than 4700 citations, in January 2023. He has organized several special sessions at the meta conferences. He has co-edited the book *Transformation Wave Physics: Electromagnetics, Elastodynamics and Thermodynamics* at Pan Stanford Publishing. His research is in the fields of plasmonics and metamaterials with applications spanning optical and acoustical waves.

Dr. Farhat is an Active Reviewer for many international journals in *Physics*, including *Physical Review Letters* and *Nature Physics*.